Computers in Biology and Medicine 109 (2019) 171–181

Contents lists available at ScienceDirect

Computers in Biology and Medicine

journal homepage: www.elsevier.com/locate/compbiomed

Independent component analysis based algorithms for high-density electromyogram decomposition: Systematic evaluation through simulation

Chenyun Dai, Xiaogang Hu*

Joint Department of Biomedical Engineering, University of North Carolina at Chapel Hill, USA
North Carolina State University, USA

ARTICLE INFO

Keywords:
Biosignal processing
Electromyogram
Source separation
Independent component analysis
RobustICA
Simulation

ABSTRACT

Motor unit activities provide important theoretical and clinical insights regarding different aspects of neuromuscular control. Based on high-density electromyogram (HD EMG) recordings, we systematically evaluated the performance of three independent component analysis (ICA)-based EMG decomposition algorithms (Infomax, FastICA and RobustICA). The algorithms were tested on simulated HD EMG signals with a range of muscle contraction levels and with a range of signal quality. Our results showed that all the three algorithms can output accurate (85%–100%) motor unit discharge timings. Specifically, the RobustICA consistently showed high decomposition accuracy among the three algorithms under a variety of signal conditions, especially with a low signal quality and varying contraction levels. But the yield of decomposition of RobustICA tended to be low at high contraction levels. In contrast, FastICA tended to show the lowest accuracy, but can detect the largest number of motor units, especially at high contraction levels. Our results also showed that the computation time was similar for FastICA and RobustICA, which was shorter than Infomax. Additionally, the accuracy of each algorithm correlated moderately with the clustering index—the silhouette distance measure, and correlated strongly with the rate of agreement of the algorithm pairs. Overall, our findings provide guidance on selecting particular decomposition algorithms based on specific applications with different requirement on the accuracy/yield of the decomposition.

1. Introduction

Electromyogram (EMG) signal is the superimposition of motor unit action potentials (MUAPs) generated from motoneuron discharge events that encode activities of the spinal circuitry and reflect high level neural control signals from the brain. Motoneuron discharge activities can provide theoretical understanding of the neural control of movement [1,2], offer clinical insights into neuromuscular impairment [3–5] and also be used as an interface signal for human-machine interactions [6]. Therefore, there has been a continuous effort to extract individual motor unit (MU) discharge information from the EMG signals [7–9]. MU decomposition of the EMG signals is the process of separating the spatiotemporally superimposed MUAPs into individual MU activities. Earlier work mostly involved manual expert editing [10], and later semi-automated decomposition methods have been developed based on MUAP template-matching [9,11], using highly-selective intramuscular EMG recordings constrained at low contraction levels. These approaches can only identify a limited number of MUs, largely due to the challenge of securely resolving superimposition from a large number of active MUs.

With the help of hardware development of multi-channel surface electrodes recently [12,13], advanced decomposition algorithms have been developed that can yield a large number of MUs at a wide range of contraction levels, allowing us to perform MU analysis at the population level. One decomposition method was developed by De Luca and colleagues based on a closely spaced 5-pin sensor array [12], and the algorithm [14] uses a template-matching approach through a maximum a-posteriori probability classifier. Alternatively, different blind source separation algorithms have been used to decompose EMG signals with a large number of channels. For example, the Convolution Kernel Compensation (CKC) method has been developed to decompose high-density (HD) EMG signals [15,16], and independent component analysis (ICA) based decomposition algorithm has also been applied to HD EMG decomposition [17,18]. Although different ICA algorithms have been used for source separation in other signal modalities (e.g. EEG), FastICA in combination with CKC or with peel-off method is the only ICA-based algorithm evaluated on EMG decomposition [17,18]. Furthermore, a systematic valuation of the decomposition performance is crucial. A

* Corresponding author. University of North Carolina at Chapel Hill, 144 MacNider Hall, Chapel Hill, NC, 27599, USA.
E-mail address: xiaogang@unc.edu (X. Hu).

https://doi.org/10.1016/j.compbiomed.2019.04.033
Received 5 December 2018; Received in revised form 22 April 2019; Accepted 25 April 2019

recent study [18] used the clustering index, silhouette (SIL) distance, to evaluate the decomposition results. The rate of agreement (RoA) of different algorithms can also serve as an evaluation metric of the decomposition performance [19]. However, the reliability of these metrics has not been systematically investigated.

Accordingly, our current study examined the performance of three different ICA-based HD EMG decomposition algorithms (FastICA [20], Infomax [21], and RobustICA [22]), and systematically evaluated the performance of these three algorithms under different signal conditions, in which a large range of signal conditions (excitation level and MU firing synchronization level) and signal quality (baseline noise level) were tested. The simulated EMG with known ground truth of the discharge timings was used, and allowed us to directly assess the decomposition performance. In addition, we systematically investigated the relation among the clustering index (SIL), the RoA, and the decomposition accuracy. Our main findings revealed that (1) RobustICA was able to show a consistently high accuracy under different signal conditions, but the decomposition yield tended to be low with a large number of active MUs at high muscle contraction levels; (2) FastICA was able to detect a greater number of MUs, but with the lowest accuracy under more challenging signal conditions (i.e., low signal quality and high contraction level); and (3) the decomposed MUs with a wide range of SIL and a larger RoA (> 85%) between algorithms generally showed a high decomposition accuracy (> 90%). Overall, our findings provided boundary conditions of the different ICA-based decomposition algorithms, and offered guidance regarding the choice of the algorithm based on specific application purposes with different requirements on the accuracy/yield of the decomposition. In addition, our results also showed that SIL and RoA (being more sensitive) can be combined to predict the decomposition accuracy when applied to experimental data.

2. Materials and methods

2.1. EMG decomposition

HD EMG signal can be regarded as a convoluted mixing process of hundreds of MU spike trains with their MUAPs. To decompose the raw EMG signals in the time domain into constituent MUAP trains, different Independent Component Analysis (ICA) algorithms (FastICA [20], Infomax [21] and RobustICA [22]) were used to estimate the original MU spike trains. These three algorithms were selected because of their superior performance on the source separation of EEG signals. The overall decomposition algorithms involve six procedures:

(1) Extend the raw EMG signals by adding R delayed replicas of original signals in each channel [15].
(2) Whiten the extended signals with eigenvalue decomposition.
(3) Deconvolute the signals using ICA-based algorithms with the following:
(a) The selection of contrast function $f(\cdot)$ highly influences the convergence speed, and is mostly based on experience. In our study, the most widely used contrast function *tanh* was selected for Infomax and FastICA. However, the RobustICA solves this issue by searching for the optimal convergence step based on kurtosis: $\mu_{opt} = \text{argmax}_{\mu}|(\boldsymbol{w}_i(n) + \mu g)|$, where g is the gradient of the normalized fourth-order marginal cumulant function (refer to Ref. [22] for the details of μ and g calculation). Therefore, the RobustICA does not require a specific contrast function, and has been shown as a faster approach.
(b) The iteration process was considered converged if the measure (dot products) of non-gaussianity was less than a threshold with respect to the previous iteration ($|\boldsymbol{w}_i^T(n+1)\boldsymbol{w}_i(n) - 1| < \boldsymbol{threshold}$). The convergence threshold determines the efficiency and accuracy of the algorithm. In our study, the convergence threshold was set at 10^{-4} based on a previous study [18].
(c) $\boldsymbol{B}$ is the separation matrix, which includes all m separation vectors $[\boldsymbol{w}_1, \boldsymbol{w}_2, \ldots, \boldsymbol{w}_m]$. Both FastICA and RobustICA may converge to the same source $\boldsymbol{S}$. Therefore, an orthogonalization step [20] was performed as: $\boldsymbol{w}_i(n) = \boldsymbol{w}_i(n) - \boldsymbol{B}\boldsymbol{B}^T\boldsymbol{w}_i(n)$, which is an efficient approach to reduce the probability of convergence to the same spike train.
(4) Detect the spike trains through *k-means* clustering on the decomposed source $\boldsymbol{S}$. The clustering index SIL was calculated as a metric to evaluate the decomposition performance for further analysis. The SIL was defined as the difference of point-to-centroid distances between the within-cluster distance summation and the between-cluster distance summation normalized by the larger value of the two distance summations.
(5) Remove the duplicate MUs. The algorithm may converge repetitively to the same motor unit as well as its delayed replicas because of the extension step. If any of the two decomposed MU spike trains had more than 50% synchronized discharge events within ± 1 ms after shifting the delay and aligning the timings of the two spike trains, the MU spike train with a lower SIL was removed.
(6) Identify the common MUs. RoA was used as a metric to predict the decomposition performance, and the common MUs detected by two algorithms were identified. A MU was referred as “common MU” if both algorithms identified a MU spike train with more than 50% discharge events matched within ± 1 ms window, after adjusting a timing offset.

The RoA of the two algorithms was calculated as:

$$RoA = \frac{\#\ of\ matches}{\#\ of\ matches + NI}$$

where $\#\ of\ matches$ means the number of spike timings matches with each other within ± 1 ms window, and NI is the total number of firings not identified by either of the two algorithms.

2.2. EMG signal simulation

The multi-channel EMG mathematical model [23,24] was used to simulate the EMG signals following these three steps:

First, the individual timings of the spike train were generated based on a widely used physiologically-based motor unit pool model [25]. Briefly, the progressive MU recruitment threshold was modeled as an exponential function as a function of the excitation drive. The MU discharge rate increased linearly with the excitation level, and then plateaued when it reached the maximum firing rate. The main model parameters used here are summarized in Table 1. Discharge variations with a 10% Coefficient of Variation were added for each firing event. In addition, 0%, 10%, or 20% of the MU discharge synchronization [26] was added to different test conditions.

Second, to obtain the HD MUAP templates, the waveforms were randomly selected from a HD MUAP pool. The MUAP pool was derived from earlier experimental data [27] obtained using a HD EMG acquisition system (OT Bioelettronica, Torino, Italy). The EMG signals were acquired from forearm flexor muscles (flexor digitorum superficialis and flexor carpi radialis) at 30% and 60% maximum voluntary contraction levels, and then decomposed using previously developed

Table 1
The main parameters used for the MU spike train generation.

Parameter	Value
Total number of neurons in the pool	120
Range of recruitment threshold	30
Exponential coefficient of recruitment threshold	ln30/120
Minimum firing rate	5
Maximum firing rate of first recruited MU	35
Maximum firing rate of last recruited MU	20

FastICA combined with convolution kernel compensation (CKC) algorithm. The 8 × 8 MUAP grid of each MU was estimated by a spike trigger average algorithm [28] to construct the MUAP pool. The MUAP pool was obtained experimentally rather than through a simulation based on muscle geometric models, largely because the MUAP shapes are more realistic and can closely reflect the morphological patterns of real action potentials.

Third, one 8 × 8 HD MUAP was then convolved with a spike train to create an 8 × 8 HD MUAP train grid. In order to simulate a more realistic condition, the MUAP corresponding to each firing has a ± 10% amplitude and duration variation. Different number of MUAP train grids were then superimposed to construct the 8 × 8 noise free EMG signals. In addition, prior to the convolution, the MUAP grid was also scaled by a coefficient from a uniformly distributed random number ranging from 0.1 to 2. This amplitude scaling created a range of MUAP amplitudes that are realistic to real EMG recordings, with some MUAP amplitudes below the noise level. Then, Gaussian noise (band-pass filtered at 10–900 Hz) was added to different simulated conditions [17,29].

Intuitively, the number of MUs used for the EMG construction and the noise level determined the degree of interference from noise or from MUAPs superposition, which were the two main factors that can influence the performance of the decomposition algorithms. Therefore, we simulated a range of different signal-to-noise ratios (SNR = 5, 10, 20, and 30 dB) and different excitation levels (5%, 10%, 20%, and 50% of maximum excitation). The recruited number of MUs at 5%, 10%, 20%, and 50% of maximum excitation were 14, 38, 68, and 95, respectively. All simulated data were sampled at 2048 Hz. Examples of the simulated EMG in each condition are shown in Fig. 1A. A total of 800 trials (4 SNRs × 4 excitation levels × 50 repeated trials) were simulated for the decomposition analysis. In different repeated simulation runs, different MUAPs can be randomly drawn from the MUAP pool. Fig. 1B shows the exemplar decomposition results compared with the ground truth (only 5 MUs are shown for clarity).

To further test the performance of the algorithms under a more challenging condition, a varying mean firing rate and MUAP amplitude following a trapezoid was simulated. Under trapezoidal contraction, there is MU progressive recruitment and derecruitment, and variations in MUAP amplitudes during the ramp-up and ramp-down phases. Specifically, a 10-s trial with two trapezoidal excitatory drive profile was created with a 1-s rest period in between (Fig. 2A). The two trapezoids were simulated to test the decomposition performance when the MUs derecruit and recruit again. The MU recruitment and derecruitment thresholds were based on the excitation level described in a previous motoneuron pool model [25] (Fig. 2A). Each trapezoid had a 1-s ramp up and ramp down portion, and a 2.5-s steady portion. The entire 10-s signal involving two 4.5-s trapezoids and 1-s rest period was used for decomposition. During the ramp portion, the firing rate increased/declined linearly with the change of excitation level. In addition, the magnitude of each column of the 8 × 8 MUAP grid was multiplied by a coefficient to simulate the shift of the muscle fibers relative to the electrodes. The signal values in each column were multiplied by a different coefficient obtained from the hamming window (Fig. 2B). Therefore, the MUAP channels in the same column were multiplied by the same coefficient, while the MUAP channels in different columns were multiplied by a different coefficient. Essentially, the hamming window slid across the columns of the channels during the ramp portion with increasing/decreasing excitation level. Eight discrete points for each column were chosen from the hamming window (see green 'x' in Fig. 2B) as the coefficients to scale the MUAP amplitude. As a result, the amplitude distribution of the MUAP in the grid shifted accordingly. Fig. 2C illustrates the change of MUAP amplitude during the two trapezoid contractions. Depending on the location of the channel, the MUAP amplitude may increase or decrease.

The goal here was not to simulate physiologically realistic changes of MUAPs, but to induce large changes in MUAP amplitude that can occur during EMG recordings with varying levels of muscle contractions. With such a coefficient modification, the amplitude of the MUAPs can experience an approximate two-fold change (Fig. 2C), substantially challenging the performance of the decomposition algorithms. For the trapezoid contraction simulation, two different SNRs (10 and 20 dB) and two excitation levels (20% and 50%) were tested. Therefore, a total of 200 trials (2 SNRs × 2 excitation levels × 50 repeated trials) were simulated.

2.3. Evaluation of decomposition performance

To quantify decomposition accuracy, the true spike train of each MU was compared with all the decomposed MUs from different algorithms. The accuracy was calculated as:

$$Accuracy = \frac{\#\ of\ matches}{\#\ of\ matches + FP + FN}$$

where *# of matches* means the number of spike timings matches with the truth within ± 1 ms window; *FP* is the number of false positive firings and *FN* is the number of false negative firings.

The RoA between algorithms was also calculated as the number of matched spikes divided by the sum of matched and unmatched spikes from either algorithm. Only MUs with a SIL > 0.5 were used for further analysis, and MU pairs with a RoA > 60% were considered common MUs.

2.4. Algorithm comparison

We first verified the optimal extension factors *R*, and the influence of synchronization level for each algorithm. The performance (accuracy and yield) of the three algorithms were quantified in the steady contraction condition, under 20 SNR with different excitation levels or synchronization levels. Second, we investigated the decomposition performance and the corresponding computation time under different SNRs and different excitation levels with the optimal *R* value and the moderate synchronization level fixed at 10%. The decomposition accuracy was correlated with the SIL and the RoA between algorithms. Lastly, we tested the influence of MUAP amplitude variation on decomposition during trapezoid force levels. The performance of the algorithms were tested statistically using repeated measures analysis of variance (ANOVA) in SPSS (IBM). To satisfy the normal distribution assumption of the ANOVA and the regression analysis, arcsine-square-root transformation was performed on the accuracy and the RoA of the decomposition. *Post hoc* pair-wise multiple comparisons were conducted with Bonferroni correction when necessary. A significance level of $p < 0.05$ was used.

3. Results

A total of 800 steady contraction trials and a total of 200 trapezoid contraction trials were simulated for algorithm evaluations.

3.1. Extension factor R verification

First, we identified the optimal extension factor *R* for each algorithm under steady contraction simulation. The *R* value was evaluated from 2 to 16 under three different synchronization levels (0%, 10% and 20%) with four different excitation levels at SNR = 20. A previous study has shown that the accuracy and the yield of the decomposition tended to increase initially, and then plateaued with a larger *R* (extended to 500 channels or more) [16]. However, the computation time increased substantially, due to the complexity of matrix operations from increased matrix size. Therefore, a lower *R* value was typically preferred when the performance (accuracy and yield) started to plateau. Our results showed that the optimal *R* value of FastICA and Infomax was consistent with the previous study, but the optimal *R* value of

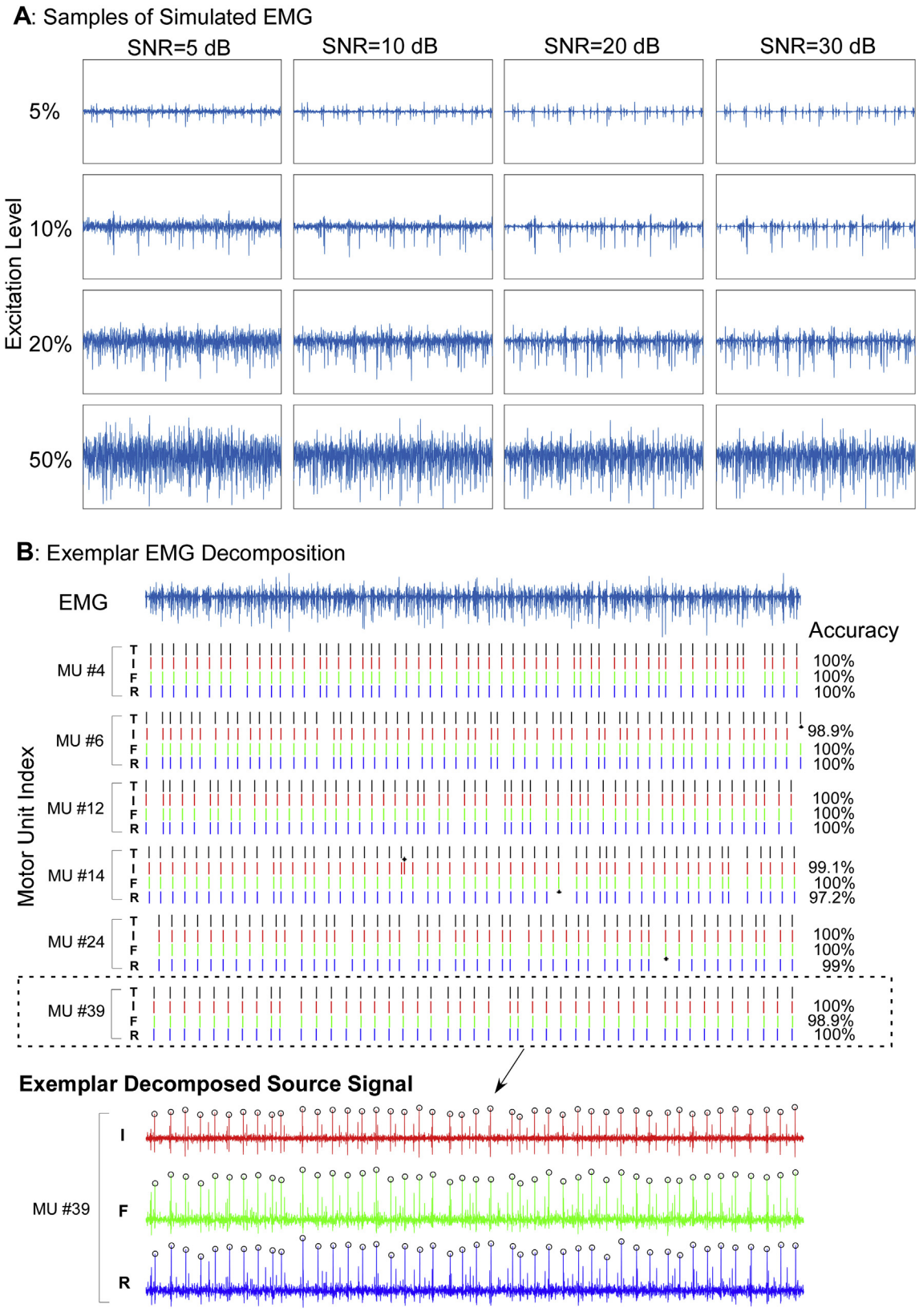

Fig. 1. A: The samples of simulated data with 1 s duration under 10% MU synchronization level. Each row represents a different excitation level. Each column represents a different signal-to-noise ratio (SNR). **B**: Exemplar EMG decomposition results compared with the ground truth (T) under 20% excitation, 20 SNR, and 10% synchronization condition. The black spikes represent the truth. The red, green, and blue spikes represent the decomposition results of the three algorithms: Infomax (I), FastICA (F), and RobustICA (R), respectively. The black dots represent false positive or false negative errors compared with the ground truth. The accuracy of the entire 10-s trial was also presented (only a 5-s window is shown for clarity). One exemplar decomposed source signal and discharge event detection are shown. The black circles represent the detected discharge events based on the *kmeans* clustering.

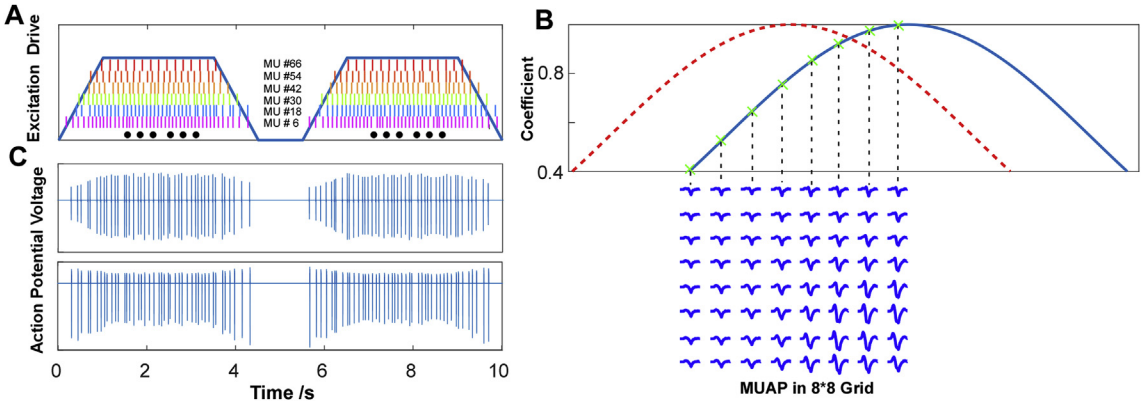

Fig. 2. EMG simulation during 20% trapezoid contraction. A: The excitatory drive profile of the trapezoid contraction. The MU progressive recruitment and de-recruitment at different excitation levels. Different colors represent different MUs. Each vertical bar represents one discharge event. Only six representative MU spike trains are shown for clarity. B: The hamming window for the modification of MUAP amplitude. During ramp-up, the solid trace shift to the red dashed trace, and shift back during ramp-down. The 'x' symbols represent the coefficient multiplied with the MUAPs in each corresponding column. C: Two examples show the change of the MUAP amplitude in the first and last channels of the 8 × 8 grid during the trapezoid contraction.

RobustICA was also affected by the synchronization level and the excitation level.

Fig. 3 shows the performance of each algorithm under different conditions. Regarding the accuracy and yield of Infomax (red dash lines) and FastICA (green solid lines), their performance showed similar trend when *R* increased from 2 to 8, and then tended to plateau after 8. For RobustICA (blue dot lines), the accuracy monotonically increased with *R*. However, the number of MUs detected dropped substantially from 8 to 16, especially when the signals contained more action potentials at high excitation levels or the correlation of sources became higher (high synchronization levels). In addition, the performance for all the three algorithms did not change with the synchronization level when the excitation levels were low to moderate (5% or 10%). However, when the synchronization level was high, the accuracy of Infomax and FastICA reduced by approximately 1–2% at 10% excitation level and 4–5% at 20% excitation level, and the number of MUs detected reduced by about 2 MUs with increasing synchronization level. In contrast, the accuracy of RobustICA did not change with the synchronization level, but the number of MUs detected substantially decreased at larger *R* values. Based on these results, 8 was chosen as the best *R* value for the rest of the analyses, and this led to a total of 576 channels after extension. Since a moderate level of MU firing synchronization was typically observed during experimental testing [26], 10% synchronization level was used for subsequent simulations.

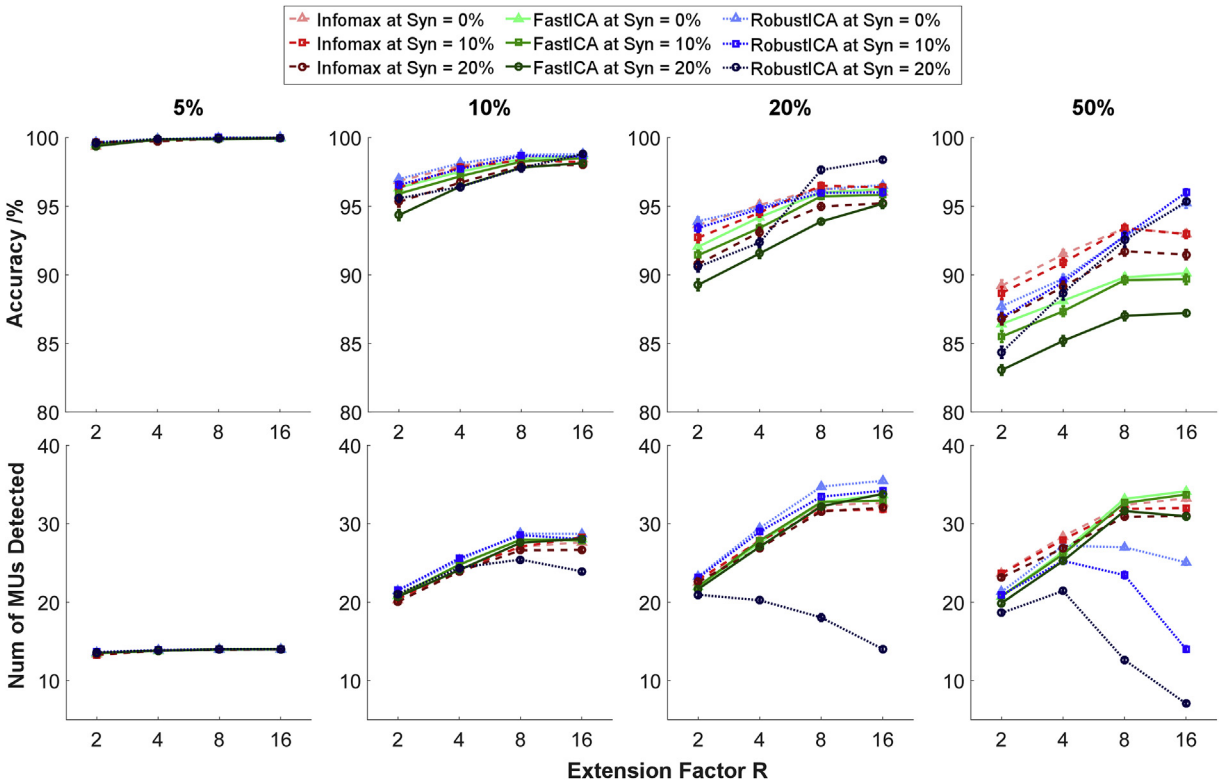

Fig. 3. Extension factor R evaluation for the three algorithms. Red dash lines: Infomax; green solid lines: FastICA; blue dot lines: RobustICA. Triangle represents 0% synchronization level. Square represents 10% moderate synchronization level. Circle represents 20% high synchronization level. Four columns from left to right are 5%, 10%, 20% and 50% excitation levels. Top row is the decomposition accuracy. Bottom row is the decomposition yields.

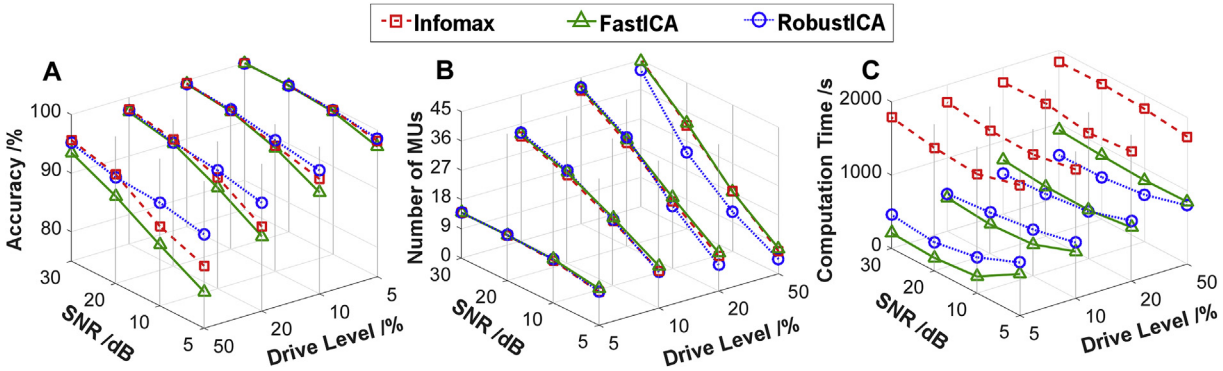

Fig. 4. The overall performance of the three algorithms under steady contraction simulation. **A**: 3-D plot of accuracy at different SNRs and excitation levels. **B**: 3-D plot of the number of MUs detected at different SNRs and excitation levels. **C**: 3-D plot of the computation time at different SNRs and excitation levels. The red dash-square lines represent Infomax. The green solid-triangle lines represent FastICA. The blue dot-circle lines represent RobustICA.

3.2. Algorithm comparison under steady contraction

The performance of the three algorithms was compared using the steady contraction simulation data under different SNRs and excitation levels (Fig. 4). Overall, we found that all the three ICA-based algorithms had a high accuracy (> 90%) under most of the simulated conditions. Even for the most challenging condition (50% excitation level with SNR = 5), the RobustICA had an accuracy at approximately 95%, and the other two algorithms had an accuracy close to 85%. In general, RobustICA showed a consistently high performance under different signal conditions in that it presented the highest accuracy when SNR was low, but detected the least number of MUs when the signals were more challenge for the algorithm (50% excitation level or SNR = 5), in comparison with the other two algorithms.

In addition, the corresponding computation time (Fig. 4C) of the three algorithms was investigated under MATLAB R2016a (MathWorks Inc.), and Intel Core i7-6700@3.40GHz with 32 GB of memory environment. Since Infomax extracted the sources concurrently by minimizing the mutual information, the decomposition runs of Infomax were selected based on the number of extended channels ($(R(8)+1) \times 64 = 576$). For fair comparison, the same number of decomposition runs was used for FastICA and RobustICA. The computation time of Infomax was much longer than that of FastICA and RobustICA. In addition, the computation time of FastICA and RobustICA tended to increase as the SNR decreased or the drive level increased. FastICA required less computation time than RobustICA at less challenging signal conditions (high SNRs and low drive levels), but required more computation time as the signals became more challenging.

To further test the performance (accuracy and yield) of the decomposition, four (5%, 10%, 20% and 50% excitation levels) individual Two-Way [*SNR* × *algorithm*] repeated measures ANOVAs were performed. A significant *SNR* × *algorithm* interaction ($p < 0.05$) was always found for all the ANOVAs. Within each algorithm, the *post hoc* comparison on the factor *SNR* showed that there was significant improvement on both the accuracy and the number of detected MUs as SNR increased ($p < 0.05$), except in a few cases: the accuracy of FastICA and RobustICA had no difference ($p > 0.05$) between SNR = 20 and 30, when the excitation level was 5%.

To compare the performance between algorithms, multiple comparisons were performed under each excitation and SNR levels. The main findings are summarized in Table 2. Overall, the accuracy of RobustICA and Infomax was higher than FastICA, but the decomposition yield of FastICA was higher than RobustICA and Infomax.

The effect of reducing the number of electrodes on the decomposition performance was also tested (Fig. 5). We compared the performance when using 64, 54, 44, 34, and 24 channels. When the channel reduction step was performed, 10, 20, 30, or 40 channels with the smallest signal power were removed for decomposition. We typically observe that a large number of channels at the edge of the electrode grid are off the muscle belly and the recordings are largely baseline noise. Depending on the muscle, the active region may be localized to a small region relative to the large electrode grid. As a result, a large number of channels will also just record baseline noise. Therefore, we reduced the channel number based on the signal amplitude in order to reduce the computation time. Three (Infomax, FastICA, and RobustICA) individual three-Way [*SNR* × *Excitation level* × *Number of channels*] repeated measures ANOVAs were performed. Besides *SNR* and *Excitation level*, a significant ($p < 0.05$) effect on the factor *Number of channels* was found without interactions for all the three algorithms. The *post hoc* comparison further revealed that the accuracy of using 64, 54, and 44 channels had no significant difference but the accuracy was higher than just using 34 or 24 channels. On the other hand, the yield was always higher when using a greater number of channels.

We also investigated the correlation among the SIL, RoA, and accuracy. Fig. 6A shows the SIL of individual MUs and the corresponding accuracy, as well as the mean accuracy at each SIL value. A moderate correlation ($R^2 = 0.69$ to 0.82) was observed based on the linear regression. Note that the linear regression was performed on the data with arcsine-square-root transformation, and then converted back to the original scale shown in the figure. Fig. 6B shows the RoA between algorithm pairs and their corresponding accuracy. We found that a high RoA (> 85%) can provide a strong confidence that both algorithms are accurate (> 90%), although a majority of the accuracy values were higher than their individual agreement values. Fig. 6C illustrates the overall relation among the three variables. When RobustICA was compared with FastICA or Infomax, the RoA was a stronger predictor of accuracy than SIL, with a high accuracy corresponding to a high RoA

Table 2
The main findings of one-way [*algorithm*] repeated measures ANOVAs for the three algorithms. **Acc** and **Num** represent accuracy and the number of MUs detected.

Excitation	If significance		Main findings
5%	**Acc**	Yes	RobustICA = Infomax > FastICA at SNR = 5 dB
	Num	Yes	FastICA > RobustICA = Infomax at SNR = 5 dB FastICA = RobustICA > Infomax at SNR = 10 dB
10%	**Acc**	Yes	RobustICA > Infomax > FastICA at SNR = 5 dB RobustICA > FastICA at SNR = 10 dB
	Num	Yes	FastICA > RobustICA = Infomax at SNR = 5 dB.
20%	**Acc**	Yes	RobustICA > Infomax > FastICA at SNR = 5 and 10 dB
	Num	Yes	FastICA > Infomax > RobustICA at SNR = 5 dB
50%	**Acc**	Yes	RobustICA > Infomax > FastICA at SNR = 5 and 10 dB RobustICA = Infomax > FastICA at SNR = 20 and 30 dB
	Num	Yes	FastICA = Infomax > RobustICA at all SNRs

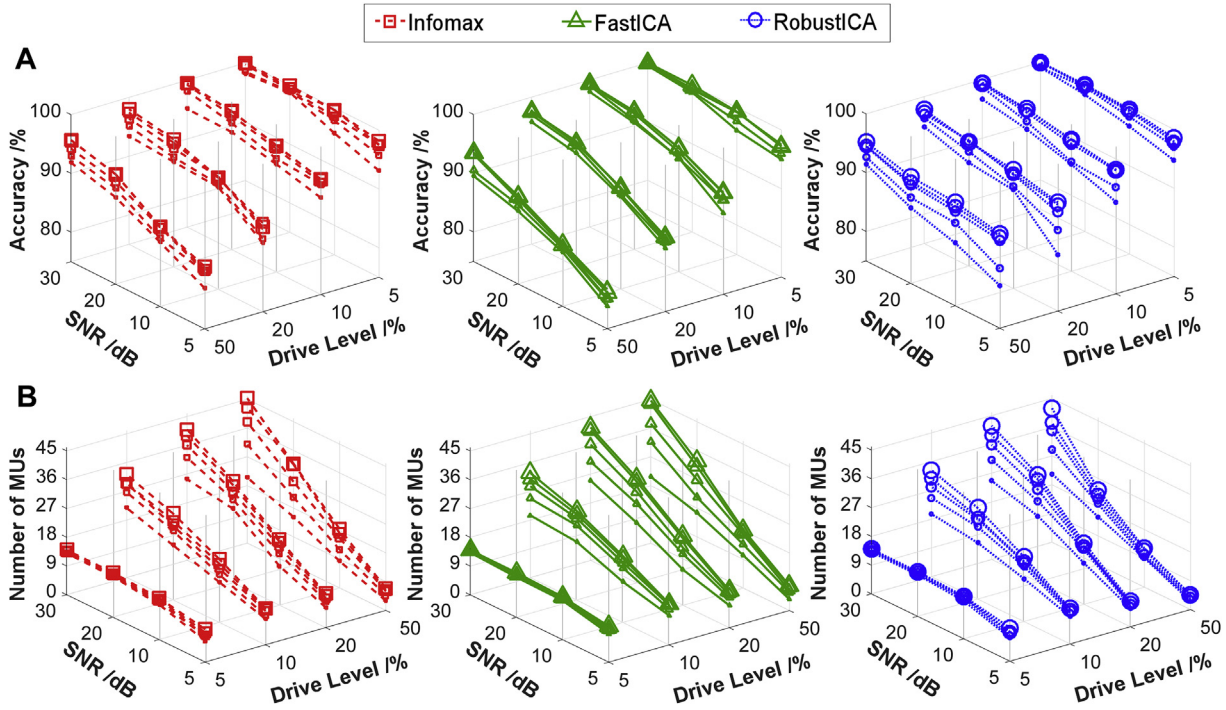

Fig. 5. The decomposition performance as the number of electrodes reduced. **A**: 3-D plot of accuracy at different SNRs and excitation levels. **B**: 3-D plot of the number of MUs detected at different SNRs and excitation levels. The red dash-square lines represent Infomax. The green solid-triangle lines represent FastICA. The blue dot-circle lines represent RobustICA. A larger symbol size represents a larger number of electrodes.

but to a wide range of SIL values. In contrast, when FastICA and Infomax were compared, only MUs with both large SIL and high RoA showed a high accuracy.

3.3. Algorithm comparison under the trapezoid contraction condition

The three algorithms were further tested in the more challenging trapezoid contraction condition. Four separate One-Way [*algorithm*] repeated measures ANOVAs were conducted in each condition. The main findings are summarized in Table 3 and Fig. 7. Overall, we found that the accuracy of RobustICA was significantly higher than Infomax and FastICA in most of the conditions ($p < 0.05$), but RobustICA detected the least number of MUs at high contraction levels ($p < 0.05$).

4. Discussion

This study evaluated the performance of three ICA-based algorithms on MU decomposition under different signal conditions using simulated EMG signals. Our results showed that all the three ICA-based algorithms can output accurate (85–100%) MU discharge timings. Specifically, the RobustICA consistently showed high accuracy among the three algorithms under a variety of signal conditions especially with a low signal quality and with varying contraction levels, but the yield of the decomposition of RobustICA tended to be low at high contraction levels. In contrast, FastICA tended to have the lowest accuracy but can detect the largest number of MUs, especially at high contraction levels. Our results also showed that the computation time was similar for FastICA and RobustICA, which was shorter than that of Infomax. With an increase in the channel number, the decomposition yield showed progressive increase, and the decomposition accuracy also increased initially but plateaued with over 44 channels. Overall, our findings provide guidance on selecting particular decomposition algorithms for specific applications with different accuracy/yield requirement. In addition, the SIL and the RoA showed varying degree of correlation with the accuracy, with RoA being a stronger predictor of accuracy, which could be used to predict the decomposition accuracy of experimental data.

4.1. ICA-based algorithms for EMG decomposition

The ICA-based algorithms used in our study differ in how the algorithms evaluate the independence of each component from the mixing signals. The three measures, including negentropy (FastICA), mutual information (Infomax), and kurtosis (RobustICA), have been widely used during independent component separation [20]. However, they may exhibit different performance depending on the properties of signal sources and mixing signals. Specifically, the negentropy-based method is commonly used due to its simplicity and fast convergence speed. However, this method is sensitive to signal artifacts [30]. Therefore, the decomposition accuracy of negentropy-based FastICA tended to be low at low SNR levels. On the other hand, the mutual-information-based Infomax can help address the artifacts issue [31]. Our decomposition results showed an improved performance of Infomax over FastICA at low SNR conditions. RobustICA is an improved kurtosis-based approach in order to address the existing issues of classic kurtosis- or negentropy-based approaches [22]. It performs an optimal search of the kurtosis contrast function instead of a random search within each iteration. Based on our results, it tended to detect the MUs with high accuracy under low SNR conditions.

All ICA-based algorithms make the assumption that the sources within the mixing signals are independent. Previous studies [32,33] have shown that MU firings have some degree of synchronization, which may affect the accuracy of source separation. On the other hand, if the MUAP trains are sparse, the ICA-based algorithm can still separate them reliably despite a low level of source synchronization. We also observed a slight decrease in the decomposition performance with a high level of firing synchronization.

4.2. Decomposition performance

With a range of simulated MUs in the EMG and with different levels of added noise or MU firing synchronization, the different ICA-based

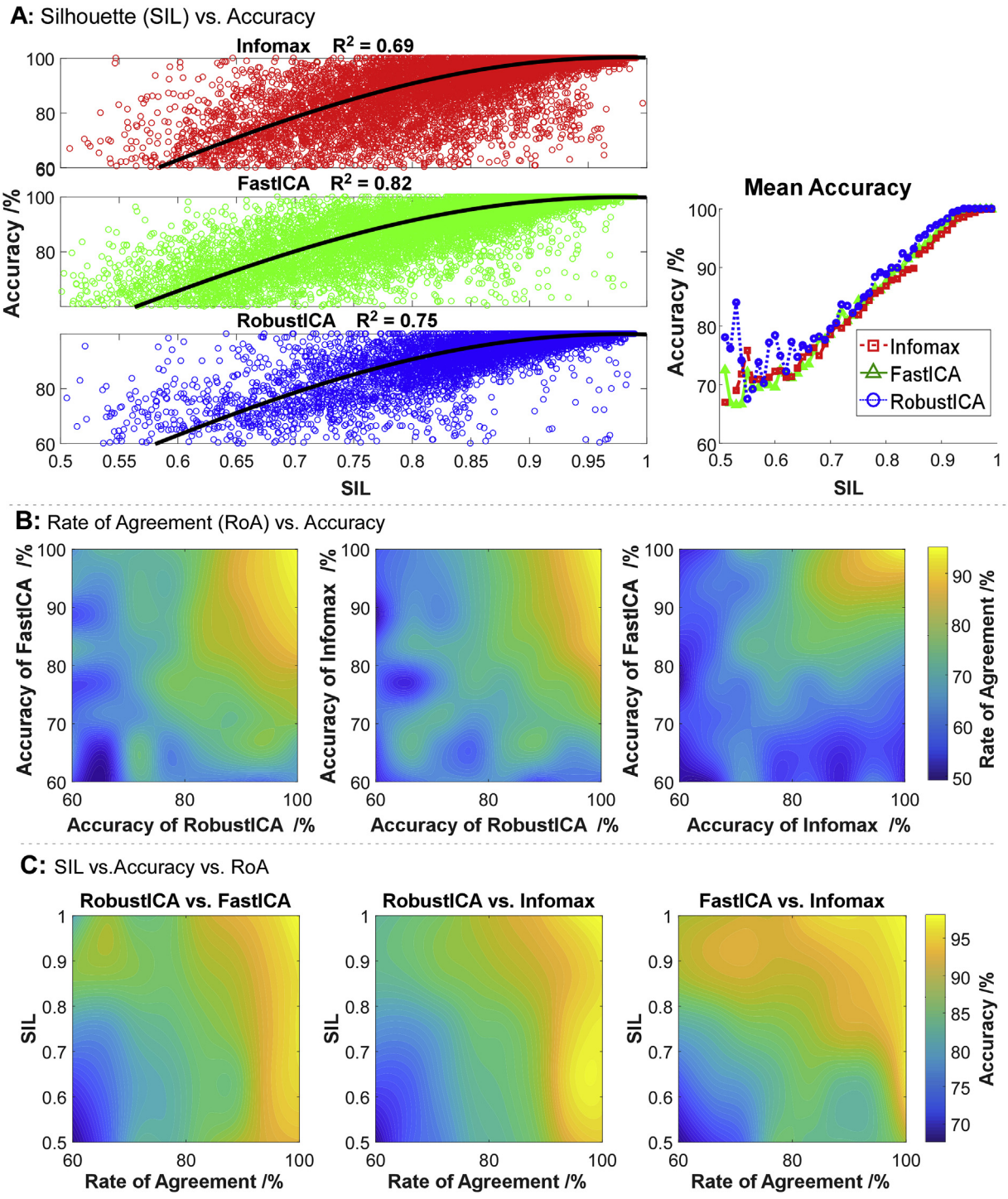

Fig. 6. A: the clustering index—silhouette measure (**SIL**) vs. the accuracy for each algorithm. Subplot 1, 2 and 3 showed the corresponding accuracy of individual motor units (MUs). Subplot on the right showed the mean accuracy. **B**: the rate of agreement (RoA) vs. the accuracy for each algorithm pair. **C**: the mean accuracy and mean SIL of two algorithms vs. the RoA of the corresponding algorithm pair.

approaches tended to give relatively accurate discharge timings in steady muscle contractions. However, as the signals contain more active MUs at higher excitation levels, a higher degree of superposition can occur. Both Infomax and FastICA tended to show less accurate decomposition outcomes compared with RobustICA, and the decomposition accuracy of FastICA was the lowest at high excitation levels even with high SNRs. In contrast, the accuracy of RobustICA was still high in these challenging conditions.

Regarding the yield of the decomposition, the number of MUs detected showed a substantial decline as the SNR decreased. The change of decomposition yield can arise from the fact that we multiplied the MUAP amplitudes by a random coefficient from a uniform distribution ranging from 0.1 to 2. Therefore, the MUAP amplitude of some MUs could be similar to or smaller than the noise level at low SNRs. As a result, those MUs may not be identified. In addition, the three algorithms have similar performance when the excitation level is less than 50%. In contrast, the performance differs when the excitation level is high, with the Infomax and FastICA giving the highest yield

Table 3
The main findings of one-way [*algorithm*] repeated measures ANOVAs for three algorithms under trapezoid conditions with MUAP amplitude variation. **Acc** and **Num** represent accuracy and the number of MUs detected.

Condition	If significance		Main findings
20% at SNR = 10 dB	Acc	Yes	RobustICA > Infomax > FastICA
	Num	Yes	FastICA > Infomax > RobustICA
20% at SNR = 20 dB	**Acc**	Yes	RobustICA > FastICA
	Num	Yes	FastICA > Infomax
50% at SNR = 10 dB	**Acc**	Yes	RobustICA > Infomax > FastICA
	Num	Yes	FastICA = Infomax > RobustICA
50% at SNR = 20 dB	**Acc**	Yes	RobustICA = Infomax > FastICA
	Num	Yes	FastICA > Infomax > RobustICA

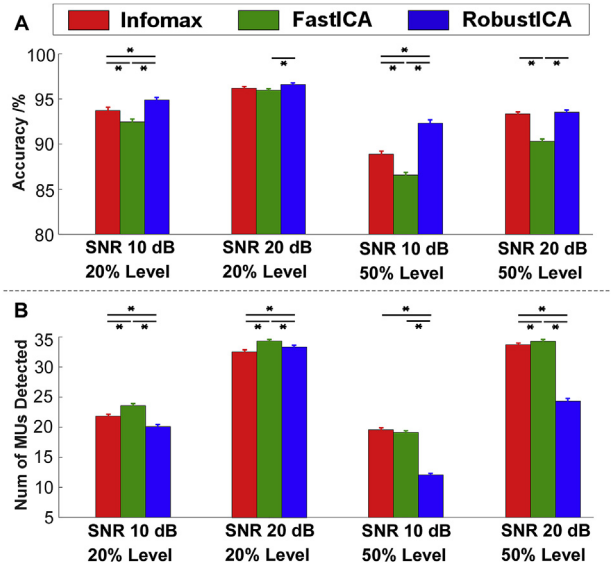

Fig. 7. The performance of the three algorithms under trapezoid conditions with MUAP amplitude variation. Red bars represent Infomax. Green bars represent FastICA. Blue bars represent RobustICA. Error bars represent the standard errors. **A**: represent the overall accuracy of the three algorithms. **B**: represent the number of MUs detected.

compared with the yield of RobustICA. It is possible that the RobustICA searches for the optimal convergence step during each iteration of separation vector calculation, which can lead to convergence to the same MUs or their replicas with high accuracy, but can lead to a smaller number of identified unique MUs. Additionally, a complete decomposition of all the simulated MUs cannot be performed in a majority of the conditions, e.g., less than 50% of MUs were decomposed out of the 95 MUs under the 50% excitation level, and less than 60% of MUs were decomposed out of the 68 MUs under the 20% excitation level. At low SNRs, approximately 10% of MUs were decomposed. A near complete decomposition was only observed when the EMG signals are relatively sparse with 5% or 10% excitation levels and with high SNRs. Nevertheless, 10–30 concurrently active MUs with a high decomposition accuracy is much higher compared with the earlier intramuscular decomposition techniques [1,34], which still allows us to evaluate the MU behavior at the population level.

Regarding the computation time, Infomax required much more computation time than FastICA and RobustICA. Since the Infomax is based on the mutual information of different sources in the mixing EMG signals, it separates different sources concurrently during each iteration step. Even if most of the extracted sources have been converged, the iteration continues until all the sources (defined by the dimension of the signals) have been converged. On the other hand, FastICA and RobustICA extracted only one source signal for each iteration, which can substantially decrease the computation time. In addition, RobustICA required less computation time as the signal became challenging, largely because RobustICA has an optimal convergence searching step, making it easier to converge for each iteration, especially for signals with a large number of sources and low SNRs [22].

Regarding the channel reduction results, the overall performance of all three algorithms decreased as the number of signal observation channels reduced. The results can rise from several aspects. ICA-based algorithms require a number of distinct observations of individual sources in order to extract each source from the mixing signals. The missing information due to reduced channel numbers can limit the decomposition performance. This is especially true for some MUs that are only recorded by a limited number of channels. With channel reduction, a majority of the information can be lost, which may lead to a lower decomposition accuracy or be completely missed by the algorithm. We also observed that the channel reduction made a greater impact on the decomposition yield than the accuracy. Specifically, the yields declined by 50% from 64 channels to 24 channels, whereas the overall accuracy only declined by up to 15% from 64 to 24 channels. The overall accuracy did not show a significant decrease until the channel number was reduced to 34. One possible reason is that the criteria of channel removal was based on the power of particular channels. The channels with a lower power mainly included MUs with small amplitude and background noise. The decomposition accuracy of MUs with small amplitudes tended to be lower. Therefore, the missed MUs by the algorithm may lead to an increment of the overall accuracy. However, the required absolute channel number for reliable decomposition likely depends on many factors: the quality of the signal (SNR and external interference, e.g., motion artifact or power line noise), the targeted muscle (superficial or deep from the skin surface, and the size of the muscle), or electrode configuration (e.g., whether the user can reconfigure the electrode placement based on the targeted muscle). To address this important issue, a careful experiment combined with simulation work is needed. A range of different muscles should be recorded with different signal quality, and associated EMG simulation should be performed that reflect the different muscle features.

4.3. Metrics for accuracy prediction

We evaluated the feasibility of using SIL and RoA to predict the decomposition accuracy of individual MUs. The SIL calculation is embedded in the *kmeans* cluster calculation, requiring minimal computation time, which could be used readily to evaluate the decomposition accuracy. We found that the mean accuracy can reach 95% with a SIL threshold > 0.9, and reach > 85% accuracy with a SIL threshold > 0.8. However, a large variation in the accuracy is not explained by the SIL based on the correlation analysis. Specifically, a certain amount of MUs with a high SIL may have low accuracy. This situation can arise when the algorithm converges to large MUAPs but actually belong to different sources (MUs). If the spatial location and the magnitude of different MUAPs are similar in the mixing signals (EMG), the ICA-based algorithm cannot distinguish them. As a result, false positive and false negative errors can occur frequently in an identified MU spike train. On the other hand, spike trains of a number of MUs with relatively low SIL values (e.g. 0.6–0.7) could still be separated accurately, largely because the spatial activation of those MUs are unique from other sources, but with low MUAP amplitudes. As a result, setting a high threshold of SIL can inevitably remove a large number of accurate MUAP trains.

The RoA was then evaluated for accuracy prediction, based on the notion that the accuracy would be high if the same MUs can be separated repetitively from different algorithms. We found that the mean accuracy can reach 95% when the RoA threshold was set to 90%, and the accuracy can reach 85% with RoA > 80%. We also observed that the MUs with low SIL values (0.6–0.7) but with a high RoA (> 95%) also showed a high accuracy > 95. The RoA is more sensitive to accuracy than SIL when these three variables are compared concurrently. In a majority of the conditions, the RoA is 5–10% lower than the

corresponding accuracy values from each algorithm. This difference can arise from two factors. First, the two algorithms can have separate errors that are un-common across algorithms, which can lead to a lower RoA. This further verified that RoA could be a good metric for accuracy prediction. Second, the low agreement can arise from the fact that one algorithm may have a relatively low decomposition accuracy than the other one.

Considering both SIL and RoA measurements, the MUs with a large SIL and a high RoA provided more confidence for the decomposition accuracy. In addition, if one metric value was very high but the other was low (e.g. SIL > 0.9 with RoA < 70 or SIL < 0.7 with RoA > 95%), the decomposition results could still be accepted for certain applications that require a large number of MUs, while allowing a certain level of decomposition errors (e.g. mean firing rate calculation over a large time window).

4.4. Implications of varying contraction conditions

All the three ICA-based algorithms were further evaluated under varying muscle contraction levels. Neither the accuracy nor the yield of all the three algorithms were also strongly influenced by the changes of the MUAP amplitude variations. In our simulation, the MUAP amplitude was designed to vary by up to 100%, based on the expectation that it will impose substantial challenge to the algorithms. However, this range was more or less arbitrary, largely because we do not have concrete experimental evidence regarding the changes of MUAP amplitude during varying levels of muscle contractions. The accuracy of RobustICA was consistently higher than that of Infomax and FastICA in most of the evaluated conditions. In addition, all the three algorithms yielded similar number of MUs under less challenging signal conditions, whereas Infomax and FastICA can detect a greater number of MUs than RobustICA under more challenging conditions. These findings are largely consistent with the steady muscle contraction conditions.

4.5. Comparison with previous decomposition algorithms

To date, FastICA and CKC have been used for high-density EMG decomposition, including CKC [15], peel-off FastICA [17,35] and FastICA combined with CKC [18]. Consistent with our findings, these EMG decomposition studies found that the decomposition accuracy and the number of MUs detected tended to become lower as the number of active MUs in the EMG signals increased or SNR decreased. For example, the peel-off FastICA study [17] simulated EMG signals with 30, 70, and 91 MUs under SNR = 10 and 20 dB, which is similar to the conditions with 10%, 20%, and 50% excitation levels under the same SNRs in our study. Compared with our FastICA results, the peel-off FastICA method showed overall accuracy > 98% under all conditions, but the yield was smaller. One potential reason was that the previous study only reported MUs with accuracy > 90%, whereas our current study considered all MUs with accuracy > 60%. The high accuracy threshold can increase the overall accuracy, but decrease the yield. Another possible reason was that the simulated signals used in the current study involved MU synchronization, which can reduce the decomposition accuracy. The CKC study [15] simulated EMG signals with 10, 20, and 30 MUs under SNR = 10 and 20 dB, which is similar to our conditions with 5% and 10% excitation under the same SNRs. Similar to our study, the earlier study reported that the CKC can reach a near complete decomposition with 10 MUs in the EMG signal. The CKC decomposition performance has been further improved when combined with a cluster analysis [16].

4.6. Limitations

When using simulated data, the ground truth of the MU firings is known, and the decomposition performance can be directly evaluated. However, simulation may not fully capture all the different characteristics of the experimental signals such as the spatial and temporal varying features of action potentials. Therefore, the number of MUs decomposed in simulated data could be larger than that in experimental data. On the other hand, the number of MUs detected in the experimental data can also vary based on the characteristics of the muscle. For example, a previous study reported that the decomposition yield ranged from 11 to 19 for abductor pollicis, but ranged from 6 to 10 for vastus lateralis [36]. Our experimental data from biceps brachii and extensor digitorum communis in Part 2 showed that approximately 5–15 MUs per contraction can be identified by RobustICA, and 6–25 MUs can be identified by FastICA or Infomax [37]. With comparable SNR and muscle contraction level, the decomposition yield was similar to the simulated data as shown in this study.

During our simulation, the action potentials were derived directly from previous experimental data through a spike triggered averaging (STA) technique, rather than from a volume conductor based model with a set of parameters specifying the properties of different tissue layers. The latter could not simulate realistic action potential spatial distribution at different electrode locations, due to limited variations in geometrical shape and conductivity at different locations of different tissue layers. The changes in complex dynamic tissue properties even during isometric muscle contractions, including irregular tissue geometry changes and ununiform fiber shifts below the recording sites, can further complicate the geometric model simulations. On the other hand, the MUAPs estimated from STA can still represent realistic action potential shapes such as due to irregularity of tissue properties as in the real biological tissue. However, there is still potential bias. For example, the MUAP shapes already identified by a decomposition algorithm could be easier to be detected by other algorithms. In addition, it is worth noting that the explicit shape variations of the MUAPs was not simulated. To simulate MUAP variations as in real EMG signals, only variations in the amplitude and duration of the average MUAPs were introduced for each simulated train of MUAP, and systematic changes in MUAP amplitude during varying contraction levels were also introduced to simulate muscle fiber shift beneath the recording electrodes. Therefore, we believe that the use of STA-based MUAP in the simulation will minimize the bias of our evaluation of the decomposition accuracy compared with other simulation approaches.

5. Conclusion

Overall, through a systematic evaluation of the performance of different ICA-based algorithms on simulated EMG signals, we found that the accuracy of RobustICA was typically higher than FastICA and Infomax in a range of signal conditions, especially with a low signal quality, a high excitation level, and a varying signal condition. The yield of the decomposition of RobustICA, however, tends to be low at more challenging signal conditions, compared with the other two algorithms. Among the three algorithms, FastICA can detect the highest number of MUs under the most challenging conditions. These findings indicate that different algorithms may be selected based on specific applications. Both SIL and RoA could be used to evaluate the decomposition accuracy, and the combination of both can further decrease potential errors and provide more reliable reference about accuracy. In general, the outcomes can help us identify reliable MU activities at the population level, and provide accuracy predictions for experimental results.

Conflicts of interest

The authors have no financial relationships that may cause a conflict of interest.

Acknowledgment

This work is supported by the National Science Foundation

CBET1847319.

References

[1] J. Duchateau, R.M. Enoka, Human motor unit recordings: origins and insight into the integrated motor system, Brain Res. 1409 (2011) 42–61.

[2] C.J. De Luca, A.M. Roy, Z. Erim, Synchronization of motor-unit firings in several human muscles, J. Neurophysiol. 70 (1993) 2010–2023.

[3] C. Dai, Y. Zheng, X. Hu, Estimation of muscle force based on neural drive in a hemispheric stroke survivor, Front. Neurol. 9 (2018), https://doi.org/10.3389/fneur.2018.00187.

[4] X. Hu, A.K. Suresh, W.Z. Rymer, N.L. Suresh, Altered motor unit discharge patterns in paretic muscles of stroke survivors assessed using surface electromyography, J. Neural. Eng. 13 (2016) 046025 https://doi.org/10.1088/1741-2560/13/4/046025.

[5] C.K. Thomas, R. Bakels, C.S. Klein, I. Zijdewind, Human spinal cord injury: motor unit properties and behaviour, Acta Physiol. 210 (2014) 5–19.

[6] D. Farina, I. Vujaklija, M. Sartori, T. Kapelner, F. Negro, N. Jiang, K. Bergmeister, A. Andalib, J. Principe, O.C. Aszmann, Manmachine interface based on the discharge timings of spinal motor neurons after targeted muscle reinnervation, Nat. Biomed. Eng. 1 (2017) 25.

[7] S.H. Nawab, R.P. Wotiz, C.J. De Luca, Decomposition of indwelling EMG signals, J. Appl. Physiol. 105 (2008) 700–710.

[8] E. Chauvet, O. Fokapu, J.-Y. Hogrel, D. Gamet, J. Duchêne, Automatic identification of motor unit action potential trains from electromyographic signals using fuzzy techniques, Med. Biol. Eng. Comput. 41 (2003) 646–653.

[9] K.C. McGill, Z.C. Lateva, H.R. Marateb, EMGLAB: an interactive EMG decomposition program, J. Neurosci. Methods 149 (2005) 121–133.

[10] E.D. Adrian, D.W. Bronk, The discharge of impulses in motor nerve fibres, J. Physiol. 67 (1929) 9–151.

[11] R.S. LeFever, A.P. Xenakis, C.J. De Luca, A procedure for decomposing the myoelectric signal into its constituent action potentials-part II: execution and test for accuracy, IEEE Trans. Biomed. Eng. (1982) 158–164.

[12] C.J. De Luca, A. Adam, R. Wotiz, L.D. Gilmore, S.H. Nawab, Decomposition of surface EMG signals, J. Neurophysiol. 96 (2006) 1646–1657.

[13] R. Merletti, A. Botter, A. Troiano, E. Merlo, M.A. Minetto, Technology and instrumentation for detection and conditioning of the surface electromyographic signal: state of the art, Clin. Biomech. 24 (2009) 122–134.

[14] S.H. Nawab, S.S. Chang, C.J. De Luca, High-yield decomposition of surface EMG signals, Clin. Neurophysiol. 121 (2010) 1602–1615, https://doi.org/10.1016/j.clinph.2009.11.092.

[15] A. Holobar, D. Zazula, Multichannel blind source separation using convolution kernel compensation, IEEE Trans. Signal Process. 55 (2007) 4487–4496.

[16] Y. Ning, X. Zhu, S. Zhu, Y. Zhang, Surface EMG decomposition based on K-means clustering and convolution kernel compensation, IEEE J. Biomed. Heal. Informatics. 19 (2015) 471–477.

[17] M. Chen, P. Zhou, A novel framework based on FastICA for high density surface EMG decomposition, IEEE Trans. Neural Syst. Rehabil. Eng. 24 (2016) 117–127.

[18] F. Negro, S. Muceli, A.M. Castronovo, A. Holobar, D. Farina, Multi-channel intramuscular and surface EMG decomposition by convolutive blind source separation, J. Neural Eng. 13 (2016) 26027.

[19] C. Dai, Y. Li, A. Christie, P. Bonato, K.C. McGill, E.A. Clancy, Cross-comparison of three electromyogram decomposition algorithms assessed with experimental and simulated data, IEEE Trans. Neural Syst. Rehabil. Eng. 23 (2015) 32–40.

[20] A. Hyvärinen, E. Oja, Independent component analysis: algorithms and applications, Neural Network. 13 (2000) 411–430.

[21] A.J. Bell, T.J. Sejnowski, An information-maximization approach to blind separation and blind deconvolution, Neural Comput. 7 (1995) 1129–1159.

[22] V. Zarzoso, P. Comon, Robust independent component analysis by iterative maximization of the kurtosis contrast with algebraic optimal step size, IEEE Trans. Neural Netw. 21 (2010) 248–261.

[23] R. Merletti, L. Lo Conte, E. Avignone, P. Guglielminotti, Modeling of surface myoelectric signals. I. Model implementation, IEEE Trans. Biomed. Eng. 46 (1999) 810–820.

[24] R. Merletti, S.H. Roy, E. Kupa, S. Roatta, A. Granata, Modeling of surface myoelectric signals. II. Model-based signal interpretation, IEEE Trans. Biomed. Eng. 46 (1999) 821–829.

[25] A.J. Fuglevand, D.A. Winter, A.E. Patla, Models of recruitment and rate coding organization in motor-unit pools, J. Neurophysiol. 70 (1993) 2470–2488.

[26] W. Yao, R.J. Fuglevand, R.M. Enoka, Motor-unit synchronization increases EMG amplitude and decreases force steadiness of simulated contractions, J. Neurophysiol. 83 (2000) 441–452.

[27] C. Dai, X. Hu, Extracting and classifying spatial muscle activation patterns in forearm flexor muscles using high-density electromyogram recordings, Int. J. Neural. Syst. 29 (2019) 1850025 https://doi.org/10.1142/S0129065718500259.

[28] X. Hu, W.Z. Rymer, N.L. Suresh, Reliability of spike triggered averaging of the surface electromyogram for motor unit action potential estimation, Muscle Nerve 48 (2013) 557–570, https://doi.org/10.1002/mus.23819.

[29] A. Holobar, M.A. Minetto, D. Farina, Accurate identification of motor unit discharge patterns from high-density surface EMG and validation with a novel signal-based performance metric, J. Neural Eng. (2014), https://doi.org/10.1088/1741-2560/11/1/016008.

[30] A. Hyvärinen, Survey on Independent Component Analysis, (1999).

[31] V. Krishnaveni, S. Jayaraman, P.M.M. Kumar, K. Shivakumar, K. Ramadoss, Comparison of independent component analysis algorithms for removal of ocular artifacts from electroencephalogram, Meas. Sci. Rev. 5 (2005) 67–78.

[32] J.G. Semmler, Motor unit synchronization and neuromuscular performance, Exerc. Sport Sci. Rev. 30 (2002) 8–14, https://doi.org/10.1097/00003677-200201000-00003.

[33] A.K. Datta, J.A. Stephens, Synchronization of motor unit activity during voluntary contraction in man, J. Physiol. 422 (1990) 397–419.

[34] B. Mambrito, C.J. De Luca, A technique for the detection, decomposition and analysis of the EMG signal, Electroencephalogr. Clin. Neurophysiol. 58 (1984) 175–188.

[35] M. Chen, A. Holobar, X. Zhang, P. Zhou, Progressive FastICA peel-off and convolution kernel compensation demonstrate high agreement for high density surface EMG decomposition, Neural Plast. 2016 (2016) 3489540.

[36] A. Holobar, D. Farina, M. Gazzoni, R. Merletti, D. Zazula, Estimating motor unit discharge patterns from high-density surface electromyogram, Clin. Neurophysiol. 120 (2009) 551–562, https://doi.org/10.1016/j.clinph.2008.10.160.

[37] C. Dai, X. Hu, Independent component analysis based algorithms for high-density electromyogram decomposition: experimental evaluation of upper extremity muscles, Comput. Biol. Med. 108 (2019) 42–48 https://doi.org/10.1016/j.compbiomed.2019.03.009.